

Article

Characterization of Steric and Electronic Properties of NiNS Complexes as S-Donor Metallodithiolate Ligands

Marilyn V. Rampersad, Stephen P. Jeffery, Melissa L. Golden, Jonghyuk Lee, Joseph H. Reibenspies, Donald J. Darensbourg, and Marcetta Y. Darensbourg

J. Am. Chem. Soc., **2005**, 127 (49), 17323-17334 • DOI: 10.1021/ja055051g • Publication Date (Web): 18 November 2005

Downloaded from <http://pubs.acs.org> on March 25, 2009



More About This Article

Additional resources and features associated with this article are available within the HTML version:

- Supporting Information
- Links to the 5 articles that cite this article, as of the time of this article download
- Access to high resolution figures
- Links to articles and content related to this article
- Copyright permission to reproduce figures and/or text from this article



[View the Full Text HTML](#)



Characterization of Steric and Electronic Properties of NiN₂S₂ Complexes as S-Donor Metallodithiolate Ligands

Marilyn V. Rampersad, Stephen P. Jeffery, Melissa L. Golden, Jonghyuk Lee, Joseph H. Reibenspies, Donald J. Darensbourg, and Marcetta Y. Darensbourg*

Contribution from the Department of Chemistry, Texas A&M University, College Station, Texas 77843

Received July 26, 2005; E-mail: marcetta@mail.chem.tamu.edu

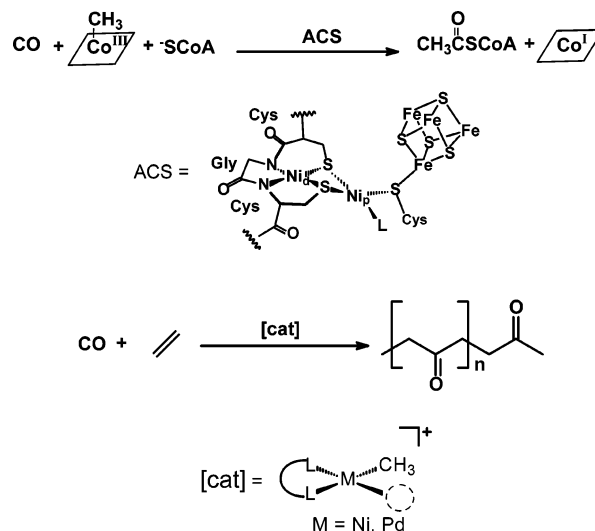
Abstract: The physical properties and structures of a series of six complexes of the type (NiN₂S₂)W(CO)₄ have been used to establish electronic and steric parameters for square planar NiN₂S₂ complexes as bidentate, S-donor ligands. According to the $\nu(\text{CO})$ stretching frequencies and associated computed Cotton–Kraihanzel force constants of the tungsten carbonyl adducts, there is little difference in donor abilities of the five neutral NiN₂S₂ metallodithiolate ligands in the series. The dianionic Ni(ema)²⁻ (ema = *N,N'*-ethylenebis(2-mercaptoacetamide)) complex transfers more electron density onto the W(CO)₄ moiety. A ranking of donor abilities and a comparison with classical bidentate ligands is as follows: Ni(ema)²⁻ > {[NiN₂S₂]⁰} > bipy ≈ phen > Ph₂PCH₂CH₂PPh₂ > Ph₂PCH₂PPh₂. Electrochemical data from cyclic voltammetry find that the reduction event in the (NiN₂S₂)W(CO)₄ derivatives is shifted to more positive potentials by ca. 0.5 V compared to the ca. -2 V Ni^{III} redox event in the free NiN₂S₂ ligand, consistent with the electron drain from the nickel–dithiolate ligands by the W(CO)₄ acceptor. Differences in Ni^{III} $\Delta E_{1/2}$ values appear to have a ligand dependence which is related to a structural feature of the hinge angle imposed by the (μ -SR)₂ bridges. Thus the angle formed by the intersection of NiN₂S₂/WS₂C₂ planes has been established by X-ray diffraction analyses as a unique orientational feature of the nickel–dithiolate ligands in contrast to classical diphosphine or diimine ligands and ranges in value from 136 to 107°. Variable-temperature ¹³C NMR studies show that the spatial orientations of the ligands remained fixed with respect to the W(CO)₄ moiety to temperatures of 100 °C.

Introduction

The development of innovative ligands for specific catalytic applications is of continuous interest in both academia and industry. Indeed the “art” of homogeneous catalysis typically lies in the minor chemical modifications of steric or electronic properties made to the ligands, such as phosphines, amines, and imines, N-heterocyclic carbenes, cyclopentadienides, and so forth, that tune a metal’s ability to control differences in rates of catalysis and product specificity.¹ The discovery of entirely new classes of ligands with unique steric demands or long-term stability toward oxidative damage motivates many synthetic efforts.

Conceivably, a recent and dramatic discovery of a new ligand class is to be found in the natural assembly of a catalytic reactive center within acetyl–CoA synthase (ACS).^{2–4} This bimetallic enzyme active site (see Scheme 1) has been deconvoluted into a nickel–dithiolate moiety, that is, a square planar NiN₂S₂

Scheme 1

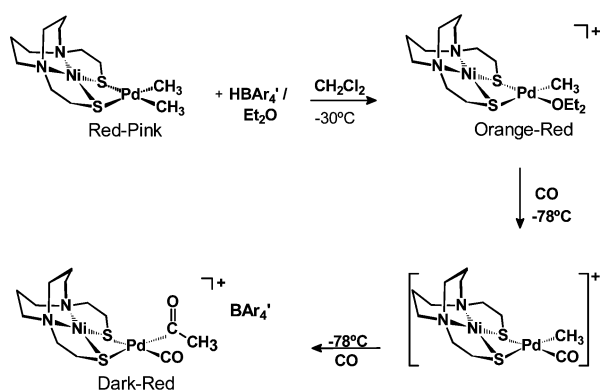


derived from a Cys–Gly–Cys tripeptide sequence within the protein, which binds a second, catalytically active nickel through bridging cysteine sulfur donors.^{2–7} The second nickel, des-

- (1) (a) Van Leeuwen, P. W. N. M. *Homogeneous Catalysis, Understanding the Art*; Kluwer Academic Publishers: Dordrecht, The Netherlands, 2004. (b) Van Leeuwen, P. W. N. M.; Kamer, P. C. J.; Reek, J. N. H.; Dierkes, P. *Chem. Rev.* **2000**, *100*, 2741–2769.
- (2) Dokov, T. I.; Iverson, T. M.; Seravalli, J.; Ragsdale, S. W.; Drennan, C. L. *Science* **2002**, *298*, 567–572.
- (3) Darnault, C.; Volbeda, A.; Kim, E. J.; Legrand, P.; Vernède, X.; Lindahl, P. A.; Fontecilla-Camps, J. C. *Nat. Struct. Biol.* **2003**, *10*, 271–279.
- (4) Svetlitchnyi, V.; Dobbek, H.; Meyer-Klaucke, W.; Meins, T.; Thiele, B.; Romer, P.; Huber, R.; Meyer, O. *Proc. Natl. Acad. Sci. U.S.A.* **2004**, *101*, 446–451.

- (5) Lindahl, P. A. *Biochemistry* **2002**, *41*, 2097–2105.
- (6) Seravalli, J.; Xiao, Y.; Gu, W.; Cramer, S. P.; Antholine, W. E.; Krymov, V.; Gerfen, G. J.; Ragsdale, S. W. *Biochemistry* **2004**, *43*, 3944–3955.

Scheme 2



ignated Ni_p in Scheme 1, mediates the assembly of the acetyl–CoA thioester from CH₃⁺ (from the corronoid cobalt–methyl donor), carbon monoxide, and the elaborate thiolate, CoA.^{8,9} The role of the first nickel, Ni_d, in N₂S₂ coordination appears to be largely structural, that is, serving as a template for the tripeptide. The bidentate NiN₂S₂ ligand thus derived has the appropriate electronic (donor) features to support the C–C and C–S coupling chemistry of the second nickel, Ni_p.

The chemistry performed by the ACS active site is related to well-known organometallic chemistry which takes place at 16-electron square planar complexes, including a current industrial process which has a remarkably similar catalytic motif involving nickel or palladium ligated with diphosphines, diimines, and mixed donor bidentate ligands. The CO/R migratory insertion that follows olefin binding to an acetyl–Ni^{II} or –Pd^{II} moiety is a key step in the homogeneous catalysis of CO/olefin copolymerization for production of polyketones.^{10–12} As shown in Scheme 1, a metal-mediated C–C coupling via migratory insertion is the function of both the biological and the industrial catalysts.

That NiN₂S₂ complexes may be used as building blocks in the design of polymetallic complexes has been demonstrated for scores of compounds in numerous structural types.^{13–20} The important reaction chemistry observed in the ACS active site pointed to the potential of the NiN₂S₂ complex as a ligand in classic organometallic chemistry.^{3,8,18} Thus in preliminary studies, summarized in Scheme 2, we synthesized the (bme-

daco)Ni complex derivative of Pd(CH₃)₂ as a stable precursor to the NiN₂S₂Pd(CH₃)(solvent)⁺ complex which readily takes up CO. The rapid CO/CH₃ migratory insertion process which followed is a prototype for the first and repeating steps in CO/olefin copolymerization reactivity.²¹ The success of this test reaction implied that mixed metal complexes that are capable of catalytic activity might be similarly constructed from an available library of NiN₂S₂ ligands. Hence, characterization of the intrinsic properties of this class of ligands is of interest.

Historically, the use of metal carbonyls as spectroscopic indicators of the electron-donating abilities of ancillary ligands has been highly successful in the development of homogeneous catalysts. Indeed, the vocabulary of organometallic chemistry that describes electronic and steric characteristics of ligands has its basis in the well-known Tolman parameters.²² While other approaches and definitions have been put forth over the years,^{23–25} those of Tolman, originally developed for monodentate phosphorus donor ligands in combination with the 16-electron Ni⁰(CO)₃ as acceptor, remain the simplest and most widely used. In fact, the validity of the use of CO stretching frequencies as measures of ligand basicity or donor ability has been challenged by results from photoelectron spectra of a series of (P–P)W(CO)₄ complexes in which Me and Ph substituents on the P-donors of diphosphines were systematically varied.^{26,27} Nevertheless, as the ν(CO) frequency values continue to be a reference point for comparisons for classical ligands, such as diphosphines, diamines, or diimines, we have prepared W(CO)₄ derivatives of bidentate NiN₂S₂ complexes and recorded their IR spectra in the ν(CO) region. X-ray crystallographic analyses detail the unique spatial characteristics of a series of NiN₂S₂ complexes as ligands to W(CO)₄. Carbon-13 NMR spectroscopic studies and electrochemical characterizations are also reported for the series.

Several examples of (NiN₂S₂)M(CO)_x complexes have been reported.^{18,28–33} From the CO stretching frequencies of a 2,3-pentanedionebis(β-mercaptoethylimino)nickel–Mo(CO)₄ complex, Kang and co-workers concluded that the NiN₂S₂ metal-dithiolate ligand was a better donor than phosphines and thioethers and similar to bipyridine.²⁸ Our own work with various complexes of the NiN₂S₂ metalthiolate ligand, (bme-daco)Ni, Ni-1, including [Ni-1]Fe⁰(CO)₄, [Ni-1]Fe^{II}(CO)₂²⁺, and [Ni-1]Mo⁰(CO)₄ complexes,^{30,31} concurred with the Kang et al. study and established that the nickel dithiolate was only slightly poorer than the free, anionic thiolate as an electron donor. In more recent efforts to synthesize model complexes

- (7) Gencic, S.; Grahame, D. A. *J. Biol. Chem.* **2003**, *278*, 6101–6110.
- (8) Webster, C. E.; Darensbourg, M. Y.; Lindahl, P. A.; Hall, M. B. *J. Am. Chem. Soc.* **2004**, *126*, 3410–3411.
- (9) Amara, P.; Volbeda, A.; Fontecilla-Camps, J. C.; Field, M. J. *J. Am. Chem. Soc.* **2005**, *127*, 2776–2784.
- (10) Sen, A. *Catalytic Synthesis of Alkene-Carbon Monoxide Copolymers and Cooligomers*; Kluwer Academic Publishers: Dordrecht, The Netherlands, 2003.
- (11) Shultz, C.; DeSimone, J.; Brookhart, M. *J. Am. Chem. Soc.* **2001**, *123*, 9172–9173.
- (12) Rix, F. C.; Brookhart, M.; White, P. S. *J. Am. Chem. Soc.* **1996**, *118*, 4746–4764.
- (13) Rao, P. V.; Bhaduri, S.; Jiang, J.; Holm, R. H. *Inorg. Chem.* **2004**, *43*, 5833–5849.
- (14) Jicha, D. C.; Busch, D. H. *Inorg. Chem.* **1962**, *1*, 872–877.
- (15) Golden, M. L.; Jeffery, S. P.; Miller, M. L.; Reibenspies, J. H.; Darensbourg, M. Y. *Eur. J. Inorg. Chem.* **2004**, 231–236.
- (16) Miller, M. L.; Ibrahim, S. A.; Golden, M. L.; Darensbourg, M. Y. *Inorg. Chem.* **2003**, *42*, 2999–3007.
- (17) Jeffery, S. P.; Lee, J.; Darensbourg, M. Y. *Chem. Commun.* **2005**, 9, 1122–1124.
- (18) Linck, R. C.; Spahn, C. W.; Rauchfuss, T. B.; Wilson, S. R. *J. Am. Chem. Soc.* **2003**, *125*, 8700–8701.
- (19) Hatlevik, O.; Blanksma, M. C.; Mathrubootham, V.; Arif, A. M.; Hegg, E. L. *J. Biol. Inorg. Chem.* **2004**, *9*, 238–246.
- (20) Harrop, T. C.; Olmstead, M. M.; Mascharak, P. K. *Chem. Commun.* **2004**, *15*, 1744–1745.

- (21) Rampersad, M. V.; Jeffery, S. P.; Reibenspies, J. H.; Ortiz, C. G.; Darensbourg, D. J.; Darensbourg, M. Y. *Angew. Chem., Int. Ed.* **2005**, *44*, 1217–1220.
- (22) Tolman, C. A. *Chem. Rev.* **1977**, *77*, 313–348.
- (23) Perrin, L.; Clot, E.; Eisenstein, O.; Loch, J.; Crabtree, R. H. *Inorg. Chem.* **2001**, *40*, 5806–5811.
- (24) (a) Koide, Y.; Bott, S. G.; Barron, A. R. *Organometallics* **1996**, *15*, 2213–2226. (b) Hirota, M.; Sakakibara, K.; Komatsuzaki, T.; Akai, I. *Comput. Chem.* **1991**, *15*, 241–248. (c) White, D.; Taverner, B. C.; Coville, N. J.; Wade, P. W. *J. Organomet. Chem.* **1995**, *495*, 41–51.
- (25) Casey, C. P.; Whiteker, G. T. *Isr. J. Chem.* **1990**, *30*, 299–304.
- (26) Bancroft, G. M.; Dignard-Bailey, L.; Puddephatt, R. J. *Inorg. Chem.* **1986**, *25*, 3675–3680.
- (27) Lichtenberger, D. L.; Jatcko, M. E. *J. Coord. Chem.* **1994**, *32*, 79–101.
- (28) Kang, D.-X.; Poor, M.; Blinn, E. L. *Inorg. Chim. Acta* **1990**, 209–214.
- (29) Yoo, J.; Ko, J.; Park, S. *Bull. Korean Chem. Soc.* **1994**, *15*, 803–805.
- (30) Chojnacki, S. S.; Hsiao, Y.-M.; Darensbourg, M. Y.; Reibenspies, J. H. *Inorg. Chem.* **1993**, *32*, 3573–3576.
- (31) Lai, C.-H.; Reibenspies, J. H.; Darensbourg, M. Y. *Angew. Chem., Int. Ed. Engl.* **1996**, *35*, 2390–2393.
- (32) Reynolds, M. A.; Rauchfuss, T. B.; Wilson, S. R. *Organometallics* **2003**, *22*, 1619–1625.
- (33) Krishnan, R.; Riordan, C. G. *J. Am. Chem. Soc.* **2004**, *126*, 4484–4485.

for the [NiFe] hydrogenase enzyme active site, Reynolds et al. concluded that the NiN₂S₂ metallothiolate ligands in [Cp**Ru*(NiN₂S₂)(CO)]⁺ are better electron donors to Ru^{II} than two monodentate PMe₃ ligands in [Cp**Ru*(PMe₃)₂(CO)]⁺ or the bidentate diphosphine, Ph₂PCH₂CH₂PPh₂, in [Cp**Ru*(dppe)(CO)]⁺.³² Other studies by Rauchfuss and co-workers and by Riordan and co-workers established that dianionic NiN₂S₂ complexes containing carboxamido nitrogens within the N₂S₂ donor environment formed dinickel complexes in which the adjacent nickel was Ni⁰ in mimicry of a possible redox level in the ACS active site.^{18,33} While such isolated reports provide a guide for expectations and design of complexes based on the metallo-ligands, the serial approach found herein broadly establishes ligating properties, including both electronic and steric properties, so that they may be generally applicable. Our study also points to the hemilability of such NiN₂S₂ ligands, a characteristic computed to be of note in the mechanism of the ACS enzyme.⁸

Experimental Section

General Methods and Materials. All solvents used were reagent grade and were purified according to published procedures under an N₂ atmosphere.³⁴ The NiN₂S₂ complexes,^{35–40} *cis*-W(CO)₄(pip)₂ (pip = piperidine),⁴¹ and complexes **1–4** were synthesized according to previously published procedures.²¹ All other chemicals were purchased from Aldrich Chemical Co. and used as received. Typically, anaerobic techniques were required, and an argon-filled glovebox and standard Schlenk-line techniques (N₂ atmosphere) were employed.

Physical Measurements. Canadian Microanalytical Services, Ltd., Delta, British Columbia, Canada, performed elemental analyses. Vis/UV spectra were recorded in DMF on a Hewlett-Packard HP8452A diode array spectrometer. Infrared spectra were recorded on a Mattson Galaxy Series 6021 FTIR spectrometer in CaF₂ solution cells of 0.1 mm path length. Photolysis experiments were performed using a mercury arc vapor, 450W UV immersion lamp purchased from Ace Glass Co. ¹³C NMR analysis was carried out with an INOVA 400 MHz Varian spectrometer.

Electrochemistry. Cyclic voltammograms were recorded on a BAS-100A electrochemical analyzer using platinum wire as counter electrode, and Ag/Ag⁺, prepared by anodizing a silver wire in a CH₃CN solution of 0.01 M AgNO₃/0.1 M *n*-Bu₄NBF₄, was the reference electrode. The glassy carbon disk (0.071 cm²) working electrode was polished with 15, 3, and 1 μm diamond pastes, successively, and then sonicated in ultrapure (Millipore) water for 10 min. The solutions were purged with argon for 5–10 min, and a blanket of argon was maintained over the solution during the electrochemical measurements. All experiments were performed in CH₃CN solutions containing 0.1 M *n*-Bu₄NBF₄ analyte at room temperature. Since the oxidation peaks for samples were overlapped with the Cp₂Fe/Cp₂Fe⁺ redox wave, Cp*₂Fe served as the internal reference. The measured potential difference between Cp₂Fe/Cp₂Fe⁺ and Cp*₂Fe/Cp*₂Fe⁺ was 505 mV. Thus, all potentials are reported relative to the normal hydrogen electrode (NHE) using Cp₂Fe/Cp₂Fe⁺ as standard (*E*_{1/2} = 0.40 V vs NHE in CH₃CN).⁴²

Syntheses of (NiN₂S₂)W(CO)₄ and (NiN₂S₂)W(CO)₅ Complexes: [N,N'-Bis-2-mercaptoethyl-N,N'-diazacycloheptane]nickel(II) tungsten tetracarbonyl, (Ni-1')W(CO)₄, (5**).** The W(CO)₄(pip)₂ (0.17 g, 0.36 mmol) in 20 mL of CH₂Cl₂ was heated to 40 °C for 10 min under a N₂ atmosphere. To this was added dropwise a yellow brown slurry of Ni-1' (0.10 g, 0.36 mmol) dissolved in 10 mL of CH₂Cl₂. The resulting red-brown solution was heated for an additional 10 min at 40 °C. The solution was stirred for a few hours at 22 °C, during which a tan-brown precipitate formed. The liquid was reduced to about 10 mL under vacuum, and the tan-brown solid was washed twice with 25 mL of benzene to remove excess piperidine and twice with 25 mL of ether. The product was dried under vacuum to yield 0.13 g, 61% of (Ni-1')W(CO)₄. X-ray quality crystals were grown by diffusion of ether into a DMF solution of the product. Anal. Calcd (found) for C₁₃H₁₈N₂-Ni₁O₄S₂W₁: C, 27.3 (26.9); H, 3.17 (3.67); N, 4.89 (5.27). Vis/UV in DMF solution λ_{max} (ε): 308 (6728), 408 (1169), 450 (985), 512 (494) nm. IR (DMF, cm⁻¹): ν(CO) 1996(w), 1873(S), 1852(m), 1817(m). ¹³C NMR (DMF): δ 211.7, 208.4, 203.8 ppm.

[N,N'-Bis-2-methylmercaptoethyl-N,N'-dimethylethylenediamine]-nickel(II) tungsten tetracarbonyl, (Ni(bmmp-dmed))W(CO)₄, (6**).** In an identical manner for **5** above, a purple solution of Ni(bmmp-dmed) was added to W(CO)₄(pip)₂ (0.15 g, 0.31 mmol). Isolation yielded 0.10 g, 53% of (Ni(bmmp-dmed))W(CO)₄. X-ray quality crystals were grown by vapor diffusion of hexane into a CH₂Cl₂ solution of the product. Anal. Calcd (found) for C₁₆H₂₆N₂Ni₁O₄S₂W₁: C, 31.1 (32.0); H, 4.25 (4.75); N, 4.54 (5.01). Vis/UV in DMF solution: λ_{max} (ε) 312 (5725), 388 (609), 440 (565) nm. IR (DMF, cm⁻¹): ν(CO) 1998(w), 1878(S), 1854(m), 1821(m). ¹³C NMR (DMF): δ 213.5, 211.7, 210.1, 202.8 ppm.

[N,N'-Bis-2-mercaptoethyl-N,N'-diazacyclooctane]nickel(II) tungsten pentacarbonyl, (Ni-1)W(CO)₅, (7**).** A sample of W(CO)₆ (0.1 g, 0.28 mmol) in 40 mL of THF under N₂ was photolyzed for 2 h to yield a yellow solution of the W(CO)₅(THF) adduct (ν(CO) = 1975, 1931, 1892 cm⁻¹). Addition of a purple slurry of Ni-1 (0.08 g, 0.28 mmol) in 20 mL of THF resulted in a red-brown solution that was stirred overnight at 22 °C. The volume was reduced in vacuo to about 10 mL; addition of ca. 40 mL of hexane produced a brown solid, which was washed with hexane (2 × 40 mL) to remove excess W(CO)₆. The solid was further purified by silica gel column chromatography with CH₂Cl₂ as the eluent to remove excess Ni-1. The solid was dried under vacuum to yield 0.12 g, 72% of (Ni-1)W(CO)₅. Anal. Calcd (found) for C₁₄H₂₆N₂Ni₁O₅S₂W₁: C, 29.3 (28.9); H, 3.28 (2.92); N, 4.56 (4.25). IR (THF, cm⁻¹): ν(CO) 2062 (w), 1974 (m), 1922 (s), 1884 (m). IR (DMF, cm⁻¹): ν(CO) 2062 (w), 1972 (w), 1922 (vs), 1874 (m).

¹³C O Enrichment. Carbon-13-enriched W(CO)₆ was prepared by addition of ¹³CO gas to a CH₂Cl₂ solution of [PPN][W(CO)₅Cl].^{43,44} From tungsten hexacarbonyl, the isotopically labeled *cis*-W(CO)_{4-*n*}-(¹³CO)_{*n*}(pip)₂ was prepared by the reported method.⁴¹ Replacement of the piperidine with the NiN₂S₂ ligand yielded the (NiN₂S₂)W(CO)_{4-*n*}(¹³CO)_{*n*} complexes. Samples containing approximately 0.05–0.07 mmol of the [(NiN₂S₂)W(CO)_{4-*n*}(¹³CO)_{*n*}] complexes in 0.7 mL of DMF were prepared under Ar and used in the VT NMR studies.

X-ray Crystal Structure Determinations. Crystal data and details for data collection and refinement are given in Table 1. The crystals were mounted on a glass fiber at room temperature for the experiment. X-ray data were obtained on a Bruker P4 diffractometer. The space groups were determined on the basis of systematic absences and intensity statistics.⁴⁵ Structures were solved by direct methods. Anisotropic displacement parameters were determined for all non-hydrogen atoms. Programs used for data collection and cell refinement: Bruker

(34) Gordon, A. J.; Ford, R. A. *The Chemist's Companion*; Wiley and Sons: New York, 1972; pp 429–436.

(35) Kruger, H. J.; Peng, G.; Holm, R. H. *Inorg. Chem.* **1991**, *30*, 734–742.

(36) Darensbourg, M. Y.; Font, I.; Pala, M.; Reibenspies, J. H. *J. Coord. Chem.* **1994**, *32*, 39–49.

(37) Mills, D. K.; Reibenspies, J. H.; Darensbourg, M. Y. *Inorg. Chem.* **1990**, *29*, 4364–4366.

(38) Smece, J. J.; Miller, M. L.; Grapperhaus, C. A.; Reibenspies, J. H.; Darensbourg, M. Y. *Inorg. Chem.* **2001**, *40*, 3601–3605.

(39) Colpas, G. J.; Kumar, M.; Day, R. O.; Maroney, M. J. *Inorg. Chem.* **1990**, *29*, 4779–4788.

(40) Grapperhaus, C. A.; Mullins, C. S.; Kozlowski, P. M.; Mashuta, M. S. *Inorg. Chem.* **2004**, *43*, 2859–2866.

(41) Darensbourg, D. J.; Kump, R. L. *Inorg. Chem.* **1978**, *17*, 2680–2682.

(42) Gagne, R. R.; Koval, C. A.; Lisensky, G. C. *Inorg. Chem.* **1980**, *19*, 2854–2855.

(43) Cotton, F. A.; Darensbourg, D. J.; Kolthammer, B. W. S. *J. Am. Chem. Soc.* **1981**, *103*, 398–405.

(44) Darensbourg, D. J.; Gray, R. L. *Inorg. Chem.* **1984**, *23*, 2993–2996.

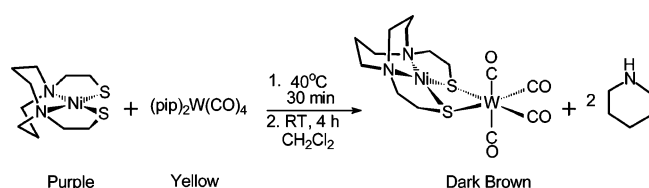
(45) Sheldrick, G. *SHELXTL-PLUS*, revision 4.11V; *SHELXTL-PLUS* users manual; Siemens Analytical X-ray Inst. Inc., Madison, WI, 1990.

Table 1. Crystallographic Data for Complexes 4–7

	4	5	6	7
formula	C ₁₄ H ₂₀ N ₂ NiO ₄ S ₂ W	C ₁₃ H ₁₈ N ₂ NiO ₄ S ₂ W	C ₁₇ H ₂₈ Cl ₂ N ₂ NiO ₄ S ₂ W	C ₁₅ H ₂₀ N ₂ NiO ₅ S ₂ W
formula weight	587.00	572.97	701.99	615.05
temperature (K)	110(2)	110(2)	110(2)	110(2)
wavelength (Å)	0.71073	0.71073	0.71073	0.71073
Z	4	4	8	4
D _{calcd} (mg/cm ³)	2.135	2.247	1.940	2.067
μ (mm ⁻¹)	7.573	8.162	5.987	7.007
crystal system	orthorhombic	orthorhombic	orthorhombic	monoclinic
space group	<i>Pnma</i>	<i>Pnma</i>	<i>Pbca</i>	<i>P2₁/n</i>
<i>a</i> (Å)	13.397(4)	12.721(5)	18.325(11)	7.2847(12)
<i>b</i> (Å)	12.386(4)	12.151(5)	12.748(7)	13.392(2)
<i>c</i> (Å)	11.005(3)	10.959(4)	20.575(12)	20.266(3)
β (°)	90	90	90	92
volume (Å ³)	1826.2(10)	1693.8(11)	4806.5(5)	1976.3(6)
goodness-of-fit	1.144	1.164	0.992	0.929
R ₁ ^a , wR ₂ ^b (%) [<i>I</i> > 2σ(<i>I</i>)]	0.0279, 0.0603	0.0719, 0.1781	0.0490, 0.1078	0.0626, 0.1403
R ₁ ^a , wR ₂ ^b (%) all data	0.0271, 0.0598	0.0800, 0.1842	0.0701, 0.1151	0.1004, 0.1558

$$^a R_1 = \sum ||F_o| - |F_c|| / \sum F_o, \quad ^b wR_2 = [\sum [w(F_o^2 - F_c^2)^2] / \sum w(F_o^2)^2]^{1/2}.$$

Scheme 3



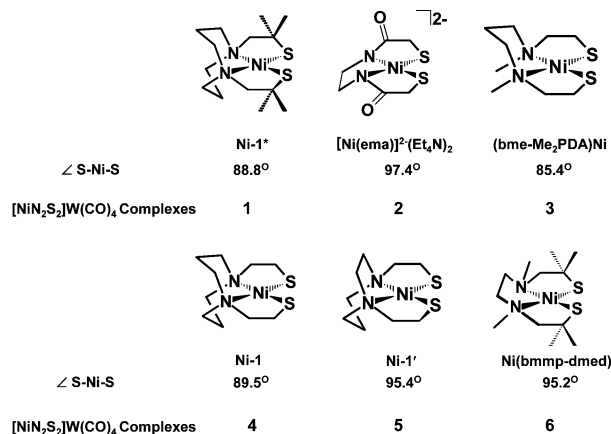
XSCANS; data reduction, SHELXTL; structure solution, SHELXS-97⁴⁶ (Sheldrick); structure refinement, SHELXL-97⁴⁷ (Sheldrick), and molecular graphics and preparation of material for publication, SHELXTL-Plus, version 5.1 or later (Bruker).⁴⁸

Results and Discussion

The NiN₂S₂ metallthiolate ligands selected for this study are comprised of a square planar nickel within a N₂S₂ donor set; variations in structures arise from several features. The diazacyclooctane derivatives **Ni-1** and **Ni-1*** have S–Ni–S ligand angles that are ca. 90°. The **Ni-1'**, based on diazacycloheptane framework, and the open-chain ligand derivative **Ni(bmmp-dmed)** have greater S–Ni–S ligand angles of 95°, resulting from a pinched N–Ni–N angle in both. The **Ni-1*** and **Ni(bmmp-dmed)** compounds possess gem dimethyl groups on the carbon α to the sulfur donor that should provide differences in steric and electron-donating properties of the thiolate sulfur. The **Ni(bme-Me₂PDA)** is a neutral ligand that has a S–Ni–S angle less than 90°. Finally, the dianionic **Ni(ema)²⁻** has the largest S–Ni–S ligand angle of 97° and, obviously, the chief capability for donation due to its charge. This last metallodithiolate ligand also bears the closest resemblance to the NiN₂S₂ moiety in the ACS active site.

The NiN₂S₂W(CO)₄ derivatives were synthesized according to the labile ligand or ligand displacement approach (Scheme 3);²¹ simple addition of the NiN₂S₂ complex to the W(CO)₄-(pip)₂ produced the NiN₂S₂W(CO)₄ products which were isolated as crystalline materials, typically in ≥60% yields (Chart 1).

Due to poor solubility in preferred nonpolar solvents, the ν(CO) stretching frequencies for the *cis*-L₂M(CO)₄ complexes

Chart 1. NiN₂S₂ Ligand Series (abbreviations, ∠S–Ni–S angles, and designations for W(CO)₄ derivatives)

Abbreviations:

Ni-1* = (N,N'-bis-2-mercapto-2-methylpropane-N,N'-diazacyclooctane) nickel(II)

Ni(ema) = (N,N'-ethylenebis-2-mercaptoacetamide) nickel(II)

Ni(bme-Me₂PDA) = (N,N'-dimethyl-N,N'-bis-2-mercaptoethyl-1,3-propanediamine) nickel(II)

Ni-1 = (N,N'-bis-2-mercaptoethyl-N,N'-diazacyclooctane) nickel(II)

Ni-1' = (N,N'-bis-2-mercaptoethyl-N,N'-diazacycloheptane) nickel(II)

Ni(bmmp-dmed) = (N,N'-bis-2-methyl-mercaptoethyl-N,N'-dimethylethylenediamine) nickel(II)

were measured in DMF. Although this solvent broadens the absorptions, peak maxima selected at ±3 or 4 wavenumbers produced little differences in the computed Cotton–Kraihanzel (C–K) force constants.⁴⁹ The ν(CO) values and the respective C–K force constants are reported in Table 2; for comparison, other *cis*-L₂M(CO)₄ (L = diphosphine, bipyridine; M = Mo) were prepared and their ν(CO) stretching frequencies also recorded in DMF.

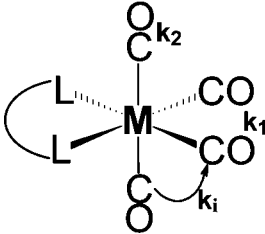
Representative infrared spectra in the ν(CO) region (Figure 1) display the four absorption bands that are expected for *cis*-L₂M(CO)₄ complexes of idealized C_{2v} symmetry, assigned to the two A₁, B₁, and B₂ vibrational modes. It should be noted that the C_{2v} symmetry designation only holds for the immediate S₂(CO)₄ donor environment about W; the significant asymmetry deriving from the hinge of the NiN₂S₂ ligand reduces the symmetry to C_s. Assuming C_{2v} symmetry, the CO stretching vibrational mode assignments are according to that of Cotton and Kraihanzel: A₁¹ corresponds to the band with the highest stretching frequency; B₁ has the greatest intensity with a

(46) Sheldrick, G. *SHELXS-97 Program for Crystal Structure Solution*; Universität Göttingen, Germany, 1997.

(47) Sheldrick, G. *SHELXL-97 Program for Crystal Structure Refinement*; Universität Göttingen, Germany, 1997.

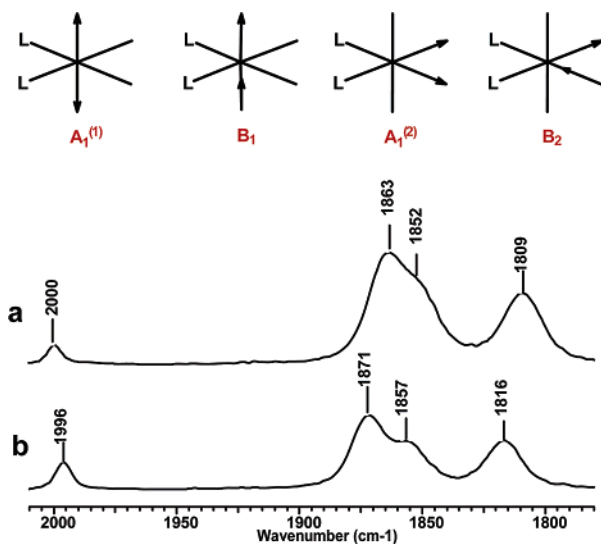
(48) *SHELXTL*, version 5.1 or later; Bruker Analytical X-ray Systems: Madison, WI, 1998.

(49) Cotton, F. A.; Kraihanzel, C. S. *J. Am. Chem. Soc.* **1962**, *84*, 4432–4438.

Table 2. CO Stretching Frequencies (cm⁻¹)^a and Calculated Force Constants (mdyn/Å)^b


compound		$\nu(A_1')$	$\nu(B_1)$	$\nu(A_1'')$	$\nu(B_2)$	k_1	k_2	k_i
Ni(bmmp-dmed)W(CO)₄	6	1998	1878	1854	1821	13.77	15.00	0.38
(Ni-1*)W(CO)₄	1	1996	1871	1857	1816	13.74	14.99	0.43
(Ni-1')W(CO)₄	5	1996	1873	1852	1817	13.74	14.98	0.41
(Ni-1)W(CO)₄	4	1995	1871	1853	1819	13.77	14.95	0.41
Ni(bme-Me₂PDA)W(CO)₄	3	1993	1876	1843	1826	13.81	14.91	0.35
[(Ni(ema)W(CO)₄)]²⁻(Et₄N)₂	2	1986	1853	1837	1791	13.41	14.77	0.46
(Ni-1*)Mo(CO)₄	8	2002	1885	1863	1821	13.80	15.17	0.41
(Ni-1')Mo(CO)₄	9	2002	1886	1851	1824	13.81	15.10	0.37
(Ni-1)Mo(CO)₄	10	2002	1884	1861	1824	13.84	15.13	0.40
(dppm)W(CO)₄^c	11	2016	1906	1906	1870	14.50	15.43	0.38
(dppe)W(CO)₄^c	12	2015	1900	1900	1870	14.50	15.34	0.38
(dmpm)W(CO)₄^c	13	2007	1885	1885	1863	14.39	15.10	0.38
(pip)₂W(CO)₄^c	14	2000	1863	1852	1809	13.68	14.94	0.46
(bipy)W(CO)₄^c	15	2006	1886	1870	1830	13.94	15.19	0.41

^a IR spectra were recorded in DMF. ^b The convention of modes and the calculated force constants follow that of ref 49. ^c Abbreviations: dppm = bis(diphenylphosphino)methane; dppe = bis(diphenylphosphino)ethane; dmpm = bis(dimethylphosphino)methane; pip = piperidine; bipy = bipyridine.

**Figure 1.** Comparison of $\nu(\text{CO})$ infrared spectra of (a) $\text{W}(\text{CO})_4(\text{pip})_2$ and (b) $(\text{Ni-1}^*)\text{W}(\text{CO})_4$ in DMF solution.

shoulder or tail corresponding to A_1'' ; and the band of lowest frequency corresponds to B_2 .⁴⁹ In the alternate approach, based on C_s symmetry, the $\text{W}(\text{CO})_4$ unit would similarly exhibit four vibrational frequencies of symmetry $3A' + A''$. In the absence of stereoselectively ¹³C-labeled species, it is not possible to unequivocally calculate individual force constants for the two different axial CO ligands. Hence, in treating the $\text{W}(\text{CO})_4$ moiety as C_{2v} , an average axial CO force constant, k_2 , was calculated. The differentiation of axial CO groups will be addressed in a discussion of the temperature-dependent ¹³C NMR data observed for these complexes (vide infra).

Among the neutral NiN_2S_2 ligands studied, only minor differences in $\nu(\text{CO})$ stretching frequencies of the $\text{NiN}_2\text{S}_2\text{W}(\text{CO})_4$ were observed. The calculated Cotton–Kraihanzel force constants found that the k_2 values (stretching force constant of

CO ligands cis to the NiN_2S_2 sulfur donors) for all the complexes are greater than the k_1 values (force constant of CO ligands trans to NiN_2S_2 sulfur donors), consistent with the trans influence exerted by the auxiliary better donor ligands (L) in the pseudo-octahedral complex. The range of k_1 or k_2 values is small for the neutral metallothiolate ligands and indicates little differences in donor abilities. As expected, the dianionic $\text{Ni}(\text{ema})^{2-}$ derivative transfers the most electron density to the $\text{W}(\text{CO})_4$ moiety, resulting in k_1 and k_2 values of 13.41 and 14.77 mdyn/Å, respectively. These are the lowest values of any compounds listed in Table 2. The neutral NiN_2S_2 sulfur donors result in CO stretching frequencies and force constants of $\text{W}(\text{CO})_4$ units that are most like the dipiperidine-substituted analogues; they are much better donors than diphosphines.

On the basis of electrochemical results ($\text{Ni}^{\text{II/I}}$ reduction couples), the complex **Ni-1*** with gem dimethyl groups on the carbon α to the sulfur is more electron rich than is **Ni-1**.⁵⁰ Nevertheless, using the $\nu(\text{CO})$ IR data in Table 2 as a criterion for donor ability, the two metallothiolate ligands are indistinguishable. A reasonable conclusion is that the steric hindrance at sulfur prevents optimal close contact of the S-donor site of **Ni-1*** to the tungsten. Such arguments have been made for sterically bulky phosphine ligands in which the spatial requirements of the phosphines impinge on the innate electron-donating ability of the P-donor site, hence obviating a separation of steric and electronic parameters.²⁶

X-ray Crystallography. As determined by X-ray diffraction analysis, the molecular structures of complexes **4–6** are shown in Figure 2, adding to the analogous $(\text{NiN}_2\text{S}_2)\text{W}(\text{CO})_4$ complexes **1–3**, which were previously reported.²¹ Selected metric data for complexes **1–6** are listed in Table 3 along with that of the free metallothiolate ligands for comparison. The molecular structure of the monodentate $(\text{NiN}_2\text{S}_2)\text{W}(\text{CO})_5$ complex **7** is

(50) Buonomo, R. M.; Font, I.; Maguire, M. J.; Reibenspies, J. H.; Tuntulani, C.; Darensbourg, M. Y. *J. Am. Chem. Soc.* **1995**, *117*, 963–973.

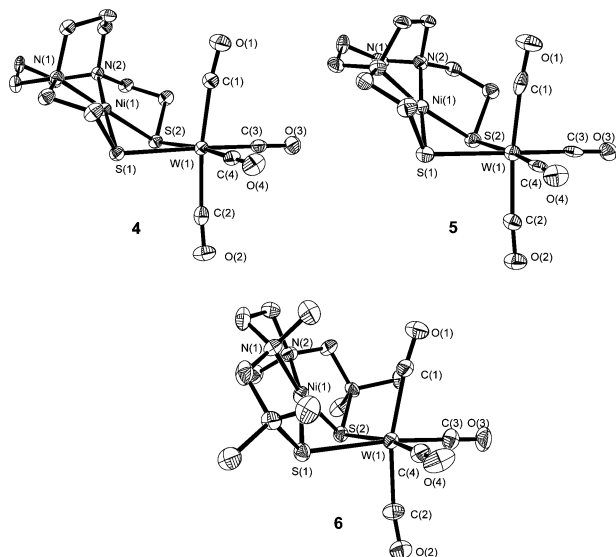


Figure 2. Thermal ellipsoid plots (50% probability) of the molecular structures for complexes **4–6** with select atoms labeled and hydrogen atoms omitted.

given in Figure 5, and a selection of distances and angles are given in the figure caption. A full list of bond lengths, bond angles, and anisotropic displacement coefficients for complexes **4–7** are in the Supporting Information.

A common characteristic of the $(\text{NiN}_2\text{S}_2)\text{W}(\text{CO})_4$ structures is that the square planar NiN_2S_2 complexes bind as bidentate, S-donor ligands to W^0 , largely maintaining the structural features of the parent NiN_2S_2 complex with only minor deviations in metric parameters. In the case of $\text{Ni}(\text{ema})^{2-}$, however, the substantially planar structure changes into one with a T_d twist of 8.6° on binding to $\text{W}(\text{CO})_4$, while the $\text{Ni-1}'$ distorts even more from planar (T_d twist of only 2.1°) to a T_d twist of 11.1° in the $(\text{Ni-1}')\text{W}(\text{CO})_4$ complex. Interestingly, the NiN_2S_2 parent (free) ligand of complex **6** has a T_d twist of 14.4° and has only a minor distortion to 16.5° on binding to $\text{W}(\text{CO})_4$.

A second notable feature of the $(\text{NiN}_2\text{S}_2)\text{W}(\text{CO})_4$ structures is that the NiN_2S_2 plane in each case connects into the $\text{S}_2\text{W}(\text{CO})_2$ plane of the pseudo-octahedral tungsten complex with a hinge at the sulfurs. This hinge, a consequence of the directionality of the sulfur lone pairs, is the hallmark of a majority of thiolate-bridged dinuclear compounds typically referred to as butterfly complexes. Rotation of the structural representation used that focuses on the octahedral geometry of the $\text{S}_2\text{W}(\text{CO})_4$ coordination sphere into a form that better displays the butterfly character of the complexes (Figure 3) illustrates the difference in the chemical environment of the two CO groups that are mutually cis to the S-donors and trans to each other. In fact, the CO that is under the $\text{Ni}\cdots\text{W}$ vector is ideally situated to be in a semibringing position. That it is strictly terminal is evident by the $\text{Ni}-\text{C}(1)$ distances in the series of six complexes, which range from 2.85 to 3.72 Å and are beyond bonding. The shorter of these actually are within the sum of Ni + C van der Waals radii ($1.63 + 1.77 = 3.33$ Å), suggesting the possibility of at least some orbital overlap. While there is no indication from $\nu(\text{CO})$ infrared data of a low frequency CO that might indicate bridging character, NMR spectroscopic studies described below find two distinct resonances for the mutually trans CO carbons.

The $\text{Ni}\cdots\text{W}$ distance range, 2.92–3.39 Å, is beyond bonding; individual values largely correlate with the dihedral angle (d.a.) made by the intersecting NiN_2S_2 and WC_2S_2 planes which cover a range of $107\text{--}136^\circ$. Inspection of the crystal packing diagrams (see Supporting Information) and metric analysis finds that, in general, the closest intermolecular nonbonding contacts, in the range of 3.08–3.2 Å, are related to carbonyl oxygen orientations toward each other between layers of the neutral complexes. In the $[\text{Et}_4\text{N}]_2[\text{Ni}(\text{ema})\text{W}(\text{CO})_4]$ salt, tetraethylammonium cations intersperse between rows comprised of pairings of interdigitated anions. We conclude that the values of the dihedral angles in the series of complexes are only influenced by intramolecular electronic and steric interactions.

Analysis of the differences in dihedral plane values benefits from comparisons of pairs of complexes in the series of six compounds. While the complexes with gem dimethyl groups on the carbon α to sulfur are expected to have the greatest spatial requirement within the $\text{W}(\text{CO})_4\text{S}_2$ coordination sphere, in fact complex **1** with d.a. = 135.6° realizes this prediction and complex **6** does not (d.a. = 114°). Inspection of the structures of complexes **1** and **6** finds a distinct difference in the orientation of the gem dimethyl groups in the two complexes (Figure 4). Whereas in complex **1**, two of the $\text{C}_\alpha\text{-CH}_3$ vectors from each of the α -carbons are parallel and pointed in the vicinity of the $\text{W}-\text{C}(1)$ bond vector, the open chain framework of complex **6** allows the analogous methyl groups to be splayed and oriented outwardly from the $\text{Ni}(\mu\text{-SR})_2\text{W}$ unit, offering little steric hindrance toward the $\text{W}(\text{CO})_4$ unit. Thus in the solid state at least, the steric encumbrance of the diazacycle-containing complex **1** is much greater than that of the open-chain complex **6**.

Complexes **4** and **5** also have large dihedral angles compared to those of other members of the series. In both cases, the C–C unit that links S to N is eclipsed across the NiN_2S_2 plane. The pucker in the five-membered NiSC_2N rings displaces the C that is α to S in each case toward the $\text{W}-\text{C}(1)$ bond vector, imposing steric hindrance from the H atoms of the $\alpha\text{-CH}_2$ groups in **4** and **5** that is nearly as great as the methyl substituent of complex **1**.

Complexes **2** and **3** have the smallest dihedral angles, 107° . The nearly flat character of the carboxamido N to S linkers accounts for the small steric requirement of complex **2**. The open-chain SNNS ligand of **3** finds the $\text{CH}_2\text{-CH}_2$ units connecting N to S eclipsed across the NiN_2S_2 plane; however, unlike complexes **4** and **5**, both carbons α to S in the NiSC_2N five-membered rings are oriented down and away from the $\text{W}-\text{C}(1)$ region. Hence, there is no obvious steric hindrance from the hydrogen atoms on that carbon.

There is no apparent correlation of dihedral or hinge angle with other metric data of the complexes such as the S–W–S bite angle or W–S distances. The former ranges from 69 to 75° deriving from S–Ni–S angles of 83 to 98° . In all members of this series, the S–Ni–S angle decreases (by 1 to 4°) upon binding of the NiN_2S_2 ligand to tungsten, forming the $\text{W}(\text{CO})_4$ derivatives (Table 3).

Minor differences in metric data exist in the Ni–S distances in members of the series of Ni–W bimetallics as compared to the free NiN_2S_2 ligands (see Table 3). Taken individually, these differences would not be statistically significant. From the series, however, the consistent observation of a slight increase in Ni–S bond length upon complexation to W, along with a concomitant

Table 3. Selected Bond Distances (Å) and Bond Angles (Deg) of Complexes 1–6 and Ball-and-Stick Representations with NiN₂S₂ Ligands Included for Comparison

	1	Ni-1* ref 36	2	[Ni(ema)] ²⁻ ref 35	3	Ni(bme-Me ₃ PDA) ref 39	4	Ni-1 ref 37	5	Ni-1* ref 38	6	Ni(bmmp-dmed) ref 40
Ni–W	3.389		2.928		3.033		3.35		3.249		3.021	
Ni–C(1)	3.726		2.954		2.846		3.561		3.388		3.24	
W–C(1)	2.001(14)		1.978(13)		2.023(13)		2.023(15)		2.03(4)		2.052(9)	
W–C(2)	2.037(12)		2.042(12)		2.047(12)		2.047(11)		2.03(8)		2.040(9)	
W–C(3)	1.951(10)		1.939(12)		1.952(8)		1.957(6)		1.96(15)		1.970(9)	
W–C(4)	1.951(10)		1.937(12)		1.952(8)		1.957(6)		1.96(15)		1.944(9)	
W–S ^a _{avg}	2.589(3)		2.616(3)		2.591(2)		2.5792(14)		2.5730(18)		2.621(2)	
Ni–S ^a _{avg}	2.170(3)		2.172(3)	2.179(1)	2.190(2)	2.175(1)	2.1893(15)	2.159(3)	2.17(16)	2.164(1)	2.155(2)	2.153(10)
Ni–N ^a _{avg}	1.986(8)		1.845(8)	1.857(3)	1.995(6)	2.005(3)	1.974(5)	1.979(7)	1.93(14)	1.940(4)	1.994(7)	1.940(3)
C(1)–W–C(2)	165.5(5)		176.5(5)		170.0(4)		172.4(3)		172.6(10)		165.5(3)	
C(3)–W–C(4)	91.3(6)		90.8(5)		89.9(4)		90.7(3)		91(9)		91.3(4)	
W–C(1)–O(1)	171.5(13)		173.4(11)		172.9(9)		171.7(7)		174.7(11)		173.8(8)	
W–C(2)–O(2)	173.3(12)		179.3(11)		170.8(8)		175.5(8)		174.9(10)		178.8(8)	
S(1)–W–S(2)	70.92(12)		75.06(9)		68.75(9)		72.08(6)		75(8)		71.16(6)	
S(1)–Ni–S(2)	87.62(15)		94.42(11)	97.44(8)	83.83(11)	85.37(4)	87.76(8)	89.4(1)	92(9)	95.4(1)	91.49(9)	95.16(4)
N(1)–Ni–N(2)	92.2(5)		86.04(4)	85.6(2)	98.3(4)	97.3(1)	91.5(3)	89.3(4)	83(7)	82.5(2)	89.8(3)	88.11(12)
dihedral ^b	135.9		107		106.8		132.5		127.5		114.4	

^a Averaged bond distances and estimated standard deviations are given in parentheses. ^b Angle between best planes of NiN₂S₂ and S₂W(CO)₂.

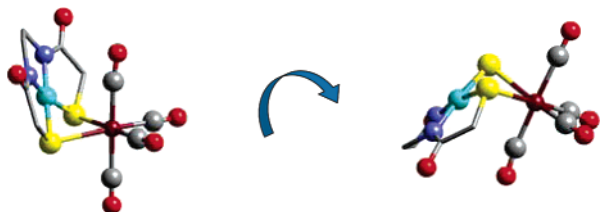


Figure 3. The butterfly core defined by the $(\mu\text{-SR})_2$ bridge in complex **2**.

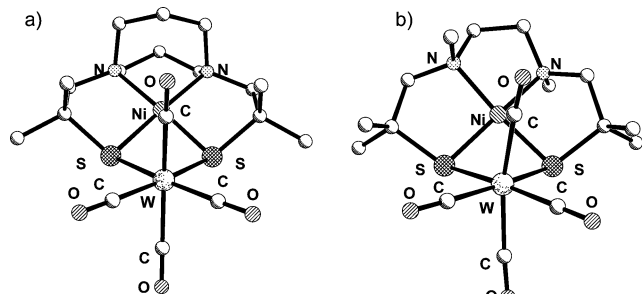


Figure 4. Ball-and-stick representations of alternate views for (a) $(\text{Ni-1}^*)\text{W}(\text{CO})_4$ and (b) $(\text{Ni}(\text{bmmp-dmed}))\text{W}(\text{CO})_4$, complexes **1** and **6**, with focus on the orientation of the gem dimethyl groups of the carbons α to the S-donor atoms—the origin of the steric difference in the two molecules as displayed in the $\text{NiN}_2\text{S}_2/\text{WS}_2\text{C}_2$ dihedral or hinge angles: 136° for the former and 114° for the latter.

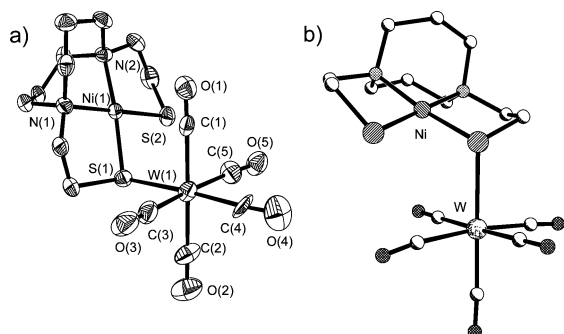


Figure 5. Two views of the molecular structures of complex **7**, $(\text{Ni-1})\text{-W}(\text{CO})_5$: (a) thermal ellipsoid plot (50% probability) with atom labels and hydrogen atoms omitted, and (b) ball-and-stick drawing. Selected averaged distances (\AA) and angles (deg): Ni–S(1), 2.176(3); Ni–S(2), 2.164(3); W–S(1), 2.577(3); Ni–N_{avg}, 1.984(8); Ni \cdots W, 3.894; S–Ni–S, 88.5(11); N–Ni–N, 89.5(3); W–C(1)–O(1), 178.3(9); W–C(2)–O(2), 177.5(12); W–C(4)–O(4), 176.5(11); W–C(5)–O(5), 172.6(11); Ni–S(1)–W, 109.8(11).

decrease in Ni–N bond length from that of the precursor NiN_2S_2 , is convincing evidence of change, presumably a decrease, in Ni–S bond character in the heterobimetallics. A different result is observed for the $\text{Ni}(\text{ema})^{2-}$ metallodithiolate ligand. The Ni–S as well as the Ni–N distances slightly decrease (or remain the same) on binding to W. The greater Ni(d_{π})–S(p_{π}) antibonding interaction in the dianionic complex and its partial relief on binding to tungsten could account for enhanced bonding in the Ni–W complex. The W–S bond distance in the $[\text{Ni}(\text{ema})\text{W}(\text{CO})_4]^{2-}$ complex **2** of 2.616 \AA is, however, within the range of that of the neutral compounds, 2.58 to 2.62 \AA .

Crystals of complex **7** were obtained inadvertently during crystallization attempts for complex **4**. Complex **7** was subsequently prepared by the labile ligand approach from the $\text{W}(\text{CO})_5$ –(THF) adduct. Views of its molecular structure are given in Figure 5. The square planar NiN_2S_2 complex is again largely unchanged from that of the parent free ligand (least-squares

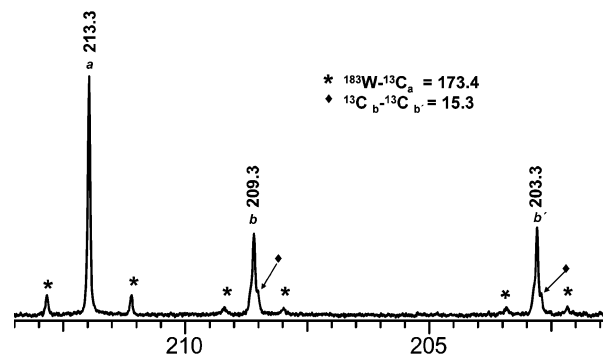


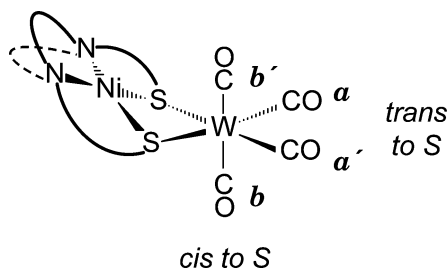
Figure 6. ^{13}C NMR spectrum of $(\text{Ni-1})\text{W}(\text{CO})_4$ in DMF at 22°C in the low-field CO region. Asterisks (*) indicate ^{183}W satellites and, ♦ indicate ^{13}C – ^{13}C coupling. Assignments refer to the structure shown in Table 4.

plane deviation of Ni, N, and S = 0.0698 \AA), and the thiolate pendant arms are in the eclipsed position. The monodentate binding of the Ni-1 unit to W produces a long Ni–W metal distance of 3.89 \AA , resulting from a W–S–Ni angle of 109.8° . At 2.176 \AA , the Ni–S(1) distance for the tungsten-bound thiolate of **7** is 0.01 \AA larger than that of the unbound Ni–S(2), 2.164 \AA .

Within the Ni-1 unit of complex **7**, both Ni–S bond distances are increased as compared to those for the free Ni-1 ligand (2.159 \AA). Both are shorter than the Ni–S_{avg} = 2.189 \AA observed in the $(\text{Ni-1})\text{W}(\text{CO})_4$ complex. The W–S_{avg} distance of $(\text{Ni-1})\text{W}(\text{CO})_4$, 2.579 \AA , is the same as that in $(\text{Ni-1})\text{-W}(\text{CO})_5$, 2.577 \AA . Only one W–C–O linkage deviates significantly from linearity (172.6°), and it is that closest to the unbound thiolate. Nevertheless, the S(2)–C(5) and S(2)–O(5) distances of 3.485 and 3.331 \AA , respectively, are beyond bonding interactions.

^{13}C NMR Spectroscopy. The ^{13}C NMR spectra of complexes **1–5**, recorded at room temperature (22°C) in DMF solvent on both natural abundance and randomly enriched C-13 samples, display three signals in the M–CO region of the spectrum in approximately 2:1:1 intensity ratio; as an example, the spectrum of complex **4** is shown in Figure 6. Chemical shifts for all complexes are listed in Table 4. The most intense resonance is assigned to the equivalent CO groups mutually trans to the S-donors of the NiN_2S_2 ligands and mutually cis to each other, labeled **a** and **a'** in Table 4. Note that only for the highly unsymmetrical complex **6** are both **a** and **a'** distinct; in all others, **a** = **a'**, consistent with the mirror plane in the solid-state structures of all except complex **6**. The nonequivalence of the carbonyls labeled **b** and **b'** is imposed by the orientation of the NiN_2S_2 ligand. The assignment of **b** and **b'** to specific resonances is not straightforward. From the dependence of C-13 chemical shifts of metal-bound carbonyls on electron density displaced onto the carbons, that carbon responsible for the resonance nearest to the position of the **a/a'** carbonyl carbon is the more electron rich. Whether this CO is closest in proximity to the NiN_2S_2 plane, or opposite, in closer proximity to the remaining lone pairs on S, is, at this time, not known.

The CO carbon resonances in the carbon-13-enriched samples have satellites that derive from ^{183}W – ^{13}C and ^{13}C – ^{13}C coupling (see Figure 6 and Table 4). The coupling constants for the CO ligands trans to the thiolate donors, $J(^{183}\text{W}\text{--}^{13}\text{C})_{\text{trans-COa}}$, are on the order of 170 Hz; they are larger than the coupling constants for the nonequivalent CO ligands cis to the thiolate

Table 4. ¹³C NMR Data, 22 °C in DMF Solution (except where noted) for the Carbonyl Carbons in [(NiN₂S₂)W(CO)₄] Complexes with the CO Designations

ligand	complex	CO (trans to S)		CO (cis to S)	
		a	a'	b	b'
Ni-1*	1^a	212.2		212.0	202.8
		¹⁸³ W– ¹³ C _a (172.0)		¹⁸³ W– ¹³ C _b (129.7)	¹⁸³ W– ¹³ C _{b'} (127.7)
Ni(ema)²⁻	2^b	216.7		209.1	207.1
				¹³ C _b – ¹³ C _{b'} (15.1)	¹³ C _b – ¹³ C _{b'} (15.1)
Ni(bme-Me₂PDA)	3	213.4		210.1	204.2
Ni-1	4	213.3		209.3	203.3
		¹⁸³ W– ¹³ C _a (173.4)		¹⁸³ W– ¹³ C _b (123.2)	¹⁸³ W– ¹³ C _{b'} (127.5)
				¹³ C _b – ¹³ C _{b'} (15.3)	¹³ C _b – ¹³ C _{b'} (15.3)
Ni-1'	5^a		211.7	208.4	203.8
Ni(bmmp-dmed)	6	213.5	211.7	210.1	202.8

^a ¹⁸³W–¹³C and ¹³C–¹³C coupling measured on ¹³C-enriched compounds. ^b CD₃CN.

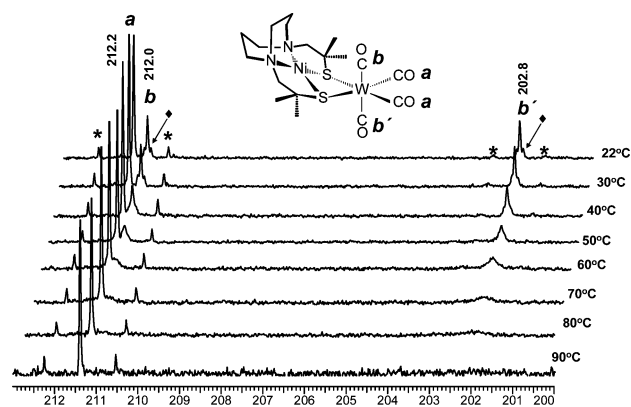


Figure 7. Variable-temperature ¹³C NMR spectra of (Ni-1*)W(CO)₄ in DMF in the low-field CO region. Asterisks (*) indicate ¹⁸³W satellites and ♦ indicate ¹³C–¹³C coupling shown in the 22 °C spectrum. Assignments of b and b' are unconfirmed.

donors: $J(^{183}\text{W}-^{13}\text{C})_{\text{cis-COb}} = 130$ Hz and $J(^{183}\text{W}-^{13}\text{C})_{\text{cis-COb}'} = 128$ Hz, respectively.⁵¹

Variable-Temperature (VT) ¹³C NMR Studies of [(NiN₂S₂)W(CO)_{4-n}(¹³CO)_n]. To determine the extent of CO site exchange in the W(CO)₄ unit, particularly whether the CO's labeled b and b' might undergo rapid interconversion of sites, the temperature dependence of C-13 NMR spectra of selected complexes in the (NiN₂S₂)W(CO)₄ series was recorded on randomly ¹³CO enriched samples dissolved in DMF. Displayed in Figure 7 are the spectra of [(Ni-1*)W(CO)_{4-n}(¹³CO)_n] measured over the range of 22 to 90 °C. The three characteristic resonances described above for complex 1 are seen in the 22 °C spectrum. The more intense resonance, which is assigned to the equivalent CO ligands trans to the thiolate donors, a, retains a narrow peak width over the temperature range. The resonances assigned to the nonequivalent CO ligands, b and b', are sharp at 22 °C, they broaden as the temperature is raised, and they coalesce into the baseline at 90 °C. At the high-temperature

limit of our experiment, 120 °C, there is evidence within the significant noise of the background at higher temperatures of the appearance of the site-averaged b + b' signal at 208.4 ppm. On cooling the sample, the resonances of b and b' reappear. Hence, we conclude that the observed CO site equilibration is a reversible phenomenon and is limited in this temperature range to the CO groups that are trans to one another.

A coalescence of resonances for carbonyls b and b' as seen for complex 1 did not occur at 90 °C or even above 100 °C for the neutral (NiN₂S₂)W(CO)₄ complexes 4 and 5. Likewise, the four resonances of complex 6 retained their integrity up to 110 °C; higher temperatures were not experimentally accessible. Analogous VT NMR studies of the dianionic complex 2 were compromised by the ring-opening of the Ni(ema)²⁻ followed by a CO redistribution process that produced a pentacarbonyl species analogous to complex 7.

Activation barriers for the (CO)_b/(CO)_{b'} site permutations in complex 1 were estimated from the following equations: $k = 1/\tau$; $\tau_{\text{coalescence}} = ((\sqrt{2})\pi\Delta\nu)^{-1}$; and $\Delta G^\ddagger = RT [\ln(R/Nh) - \ln(k/T)]$. For complex 1, the exchange rate constant was calculated at the coalescence temperature of 90 °C (363 K), and the error indicated for the activation barrier is from computations made for coalescence temperatures of ±10 on either side of 363 K.

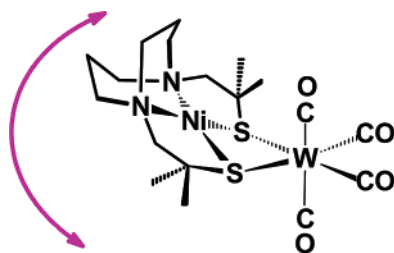
$$\tau = 2.45 \times 10^{-4} \text{ s (at 363 K)}$$

$$k = 4.08 \times 10^3 \text{ s}^{-1} \text{ (at 363 K)}$$

$$\Delta G^\ddagger = 64.4 \pm 2.0 \text{ kJ/mol}$$

The process which equilibrates the (CO)_b and (CO)_{b'} sites in complex 1 is expected to be a mutual buckling of the NiN₂S₂ and W(CO)₄ units at the sulfur hinges; alternatively, this may be described as a double inversion at the sulfurs. Notably, the molecular mobility is greatest for the complex of greatest steric encumbrance and largest hinge angle.

(51) Buchner, W.; Schenk, W. A. *Inorg. Chem.* **1984**, *23*, 132–137.



Electrochemical Studies. Cyclic voltammograms (CVs) of the $(\text{NiN}_2\text{S}_2)\text{W}(\text{CO})_4$ complexes were recorded at room temperature in CH_3CN solutions containing 0.1 M $n\text{-Bu}_4\text{NBF}_4$ as supporting electrolyte. For direct comparison, CVs of the NiN_2S_2 metallothiolate ligands were examined under identical conditions; these are overlaid with their respective $\text{W}(\text{CO})_4$ derivatives in Figure 8. The electrochemical data are summarized in Table 5.

In general, all of the neutral $(\text{NiN}_2\text{S}_2)\text{W}(\text{CO})_4$ complexes undergo one reversible reduction and one quasi-reversible oxidation within the acetonitrile solvent window. As the $(\text{pip})_2\text{W}(\text{CO})_4$ complex shows no reductions, the reversible reductions, found in the range of -1.36 to -1.64 V for complexes **1**, **3**, and **6**, are assigned as the $\text{Ni}^{\text{II/I}}$ redox couple. The shift to more positive potentials by ca. 0.50 V, as compared to the ca. -2 V $\text{Ni}^{\text{II/I}}$ redox event in the free NiN_2S_2 ligand, is compatible with formation of a Lewis base–Lewis acid adduct with the $\text{W}(\text{CO})_4$ acceptor which withdraws electron density from the metallo-ligand via the bridging thiolate sulfurs. In contrast, the oxidation event seen in the neutral NiN_2S_2 ligands in the 0.20–0.40 V range is barely changed in the $(\text{NiN}_2\text{S}_2)\text{W}(\text{CO})_4$ complexes; these were proposed to be sulfur-based in the NiN_2S_2 free ligands.⁵⁰ A second oxidative process, proposed to be nickel-based, is observed for the **Ni-1*** and **Ni(bmmp-dmed)** free ligands, but is shifted out of the CH_3CN solvent window in the $(\text{NiN}_2\text{S}_2)\text{W}(\text{CO})_4$ complexes **1** and **6**. Thus, if indeed the more accessible oxidation process is sulfur-based, it would appear to be less dependent on the formation of the $\text{W}(\text{CO})_4$ complex than are the Ni-based redox events. It should be mentioned that there is an irreversible oxidation in the CV of the $(\text{pip})_2\text{W}(\text{CO})_4$ complex at ca. +0.5 V. Hence, the assignment of the oxidation events displayed in Figure 8 is not definite.

Table 5. Half-Wave and Anodic Potentials for Reductions and Oxidations of NiN_2S_2 and $[\text{NiN}_2\text{S}_2]\text{W}(\text{CO})_4$ Complexes^a

compound	$E_{1/2}$ (V)	E_{pa} (V)	
	reduction	1st oxidation	2nd oxidation
Ni-1	-2.02	0.17	
Ni-1'	-2.03	0.21	
Ni-1*	-2.11	0.30	1.15
Ni(bmmp-dmed)	-1.97	0.38	1.04
Ni(bme-Me₂PDA)	-2.00	0.34	
[Ni(ema)](Et₄N)₂		-0.30 ^b	
(Ni-1)W(CO)₄	-1.56	0.25	
(Ni-1')W(CO)₄	-1.51	0.30	
(Ni-1*)W(CO)₄	-1.64	0.36	
Ni(bmmp-dmed)W(CO)₄	-1.42	0.35 ^c	
Ni(bme-Me₂PDA)W(CO)₄	-1.36	0.36	
[Ni(ema)W(CO)₄](Et₄N)₂	-2.34 ^d	-0.12	

^a All potentials scaled to NHE referenced to a $\text{Cp}_2\text{Fe}/\text{Cp}_2\text{Fe}^+$ standard ($E_{1/2}^{\text{NHE}} = 0.40$ V; see Experimental Section). In CH_3CN solutions, 0.1 M $n\text{-Bu}_4\text{NBF}_4$ electrolyte, glassy carbon working electrode, measured vs Ag/AgNO_3 reference electrode. ^b This oxidation peak is coupled to a return peak E_{pc} at -0.38 V. ^c This reduction peak is coupled to a return peak E_{pc} at 0.28 V. ^d This value is for an irreversible reduction peak.

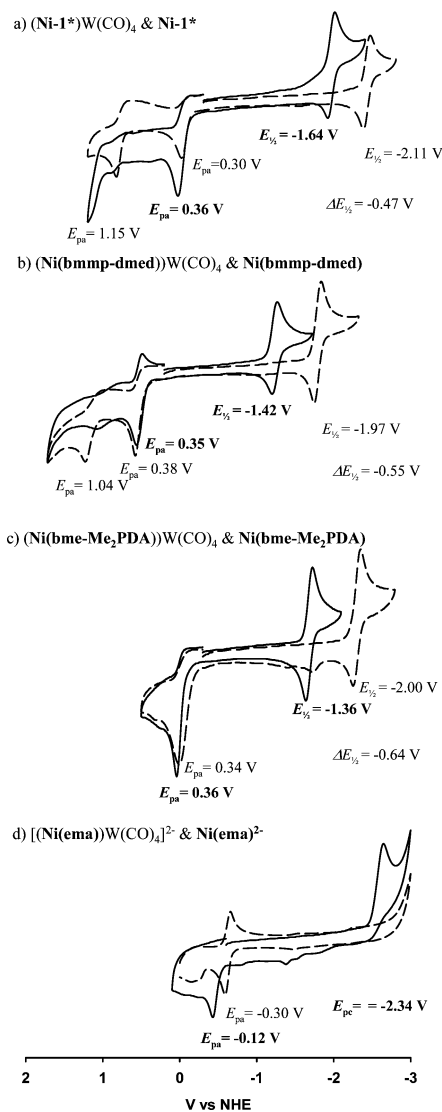


Figure 8. Cyclic voltammograms of NiN_2S_2 (dashed line) and $[\text{NiN}_2\text{S}_2]\text{W}(\text{CO})_4$ (solid line) complexes in CH_3CN solutions, 0.1 M $n\text{-Bu}_4\text{NBF}_4$ at a scan rate of 200 mV/s.

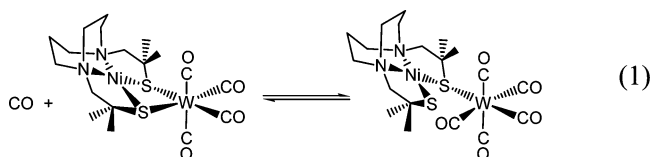
As shown in Figure 8d, the only redox event in the CV of CH_3CN solutions of $(\text{Et}_4\text{N})_2[\text{Ni}(\text{ema})]$ is a reversible oxidation at -0.30 , which earlier was assigned by Holm and co-workers to $\text{Ni}^{\text{II/III}}$; the assignment was supported by EPR spectroscopy.³⁵ In contrast, the CV of the tungsten derivative of $\text{Ni}(\text{ema})^{2-}$, $[\text{Ni}(\text{ema})\text{W}(\text{CO})_4]^{2-}$, also as its Et_4N^+ salt, reveals both an irreversible oxidation at -2.34 V under the same experimental conditions as used for study of $\text{Ni}(\text{ema})^{2-}$. Making the assumption that the complexation of the $\text{NiN}_2\text{S}_2^{2-}$ by $\text{W}(\text{CO})_4$ shifts the $\text{Ni}^{\text{II/I}}$ reduction potential at minimum by the same amount as in the neutral compounds, we estimate the $\text{Ni}^{\text{II/I}}$ reduction in the free $\text{Ni}(\text{ema})^{2-}$ to be -2.8 V or even more negative.

As the shifts in $\text{Ni}^{\text{II/I}}$ reduction potentials reflect the drain of electron density from the NiN_2S_2 coordination environment upon formation of the $\text{W}(\text{CO})_4$ adduct, one might expect a correlation of the differences in reduction potential with the $\nu(\text{CO})$ IR data. That is, the greater shift in the value $E_{1/2}$ for the $\text{Ni}^{\text{II/I}}$ couple in the **Ni(bme-Me₂PDA)** versus complex **3** as contrasted to analogous features in complex **1** would appear to indicate better

donor properties for the **Ni(bme-Me₂PDA)** ligand over the **Ni-1*** ligand. Unfortunately, the infrared and force constant data are fairly indistinguishable within the series of neutral Ni–W compounds. It is not known whether the lack of correlation of $\nu(\text{CO})$ and the Ni^{III} couple $E_{1/2}$ values is due to an inherent insensitivity of the former to small differences in donor property, or whether there should be such a correlation at all.

Stability of the (NiN₂S₂)W(CO)₄ Complexes. The neutral complexes of this type have considerable thermal stability, even in solution, as evidenced by the VT NMR studies which demonstrated complex integrity at temperatures ≥ 100 °C. With the exception of the (Et₄N)₂[**Ni(ema)**W(CO)₄], all of the NiN₂S₂W(CO)₄ are, for practical purposes, air stable.

As described above in the isolation of complex **7**, thermal decomposition of complex **4** over a 1 week period in a sealed vial, where any liberated CO could be taken up by another molecule of **4**, resulted in the pentacarbonyl species and conversion of the bidentate into a monodentate ligand. Subsequent studies of this hemilabile property with the deliberate addition of exogenous CO have shown that the pentacarbonyl complexes do not easily undergo complete CO displacement of the NiN₂S₂ ligand. Furthermore, preliminary studies find in all cases the ring closing, reformation of the tetracarbonyl, is in equilibrium with the opening/CO capture process (eq 1). The ring-opening characteristic of the Ni(μ -SR)₂W core that produces an open site on the W(CO)₄ moiety, yet persists as a nickel–thiolato ligand, is an attractive feature for catalyst design. A related scenario is prominent in the computed mechanism for the ACS enzyme activity.⁸ A kinetic study of the ring-opening process in (NiN₂S₂)W(CO)₄ complexes as they take up CO and convert to (NiN₂S₂)W(CO)₅, as defined in eq 1, is the subject of a separate report.



Summary and Comments

This detailed inspection of a series of NiN₂S₂ derivatives of W(CO)₄ has identified a unique steric property of these metallothiolate ligands to lie in the hinge angle imposed by the bridging thiolate sulfurs and their remaining quiescent lone pairs. There is no obvious correlation of the hinge angle with other metric data of the complexes such as the S–W–S bite angle or W–S distances. A detailed molecular mechanics analysis is necessary in order to assess all of the torsion angles within the polydentate ligand framework that influence the S-donor site and the dihedral or hinge angle. Nevertheless, from the crystallography data produced for this set of six complexes, we can conclude that substituents and orientations at the C_α to S produce the principal steric deviation from the inherent dihedral angle of the NiN₂S₂/S₂W(CO)₂ planes as set by the S-lone pair/W-acceptor orbital interactions. The overlay of structures in Figure 9 shows an impressive range of the steric effect seen for the W(CO)₄ series of complexes. The smallest of these is only 6° larger than the 101.3° dihedral angle observed for the **(Ni-1)**PdMeCl complex shown below.²¹ With no steric interactions possible in the two hinged square planes,

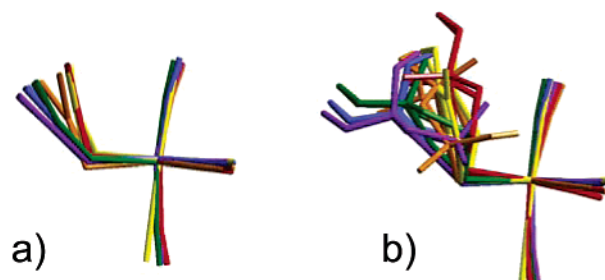
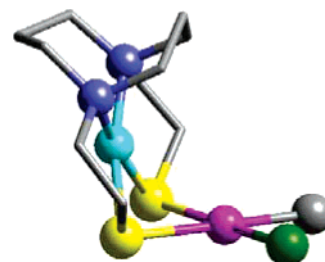
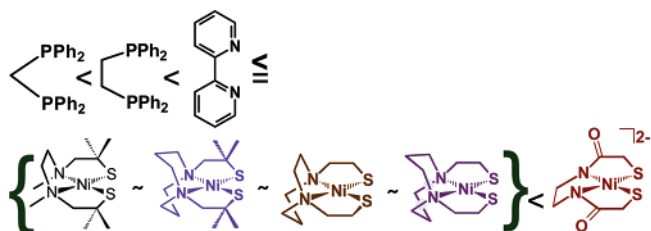


Figure 9. Structural overlay of (NiN₂S₂)W(CO)₄ complexes in order of decreasing dihedral angle with hydrogen atoms omitted: purple (**Ni-1***)-W(CO)₄, blue (**Ni-1**)W(CO)₄, green (**Ni-1'**)W(CO)₄, orange **Ni(bmmp-dmed)**W(CO)₄, yellow [Et₄N]₂[**Ni(ema)**W(CO)₄], red [**Ni(bme-Me₂PDA)**]-W(CO)₄. (a) Bond representations as cylinders using NiN₂S₂W(CO)₄ only; (b) hydrocarbons added.

the **(Ni-1)**PdMeCl complex could represent the natural dihedral angle limit for NiN₂S₂ derivatives. We have noted that such a steric effect as defined for the NiN₂S₂ ligands may become a benefit for substrate orientation in palladium-promoted coupling reactions.²¹ Importantly, the VT NMR studies establish that this orientation is fixed, even to relatively high temperatures.



The electron-donating ability of the NiN₂S₂ ligands, related to each other and to other neutral donors to a first approximation through the $\nu(\text{CO})$ stretching frequencies of W(CO)₄ adducts, finds close analogies to N-donor ligands, such as piperidine or bipyridine; the ranking is as follows:

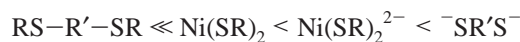


While the vibrational spectroscopy data do not distinguish between the neutral NiN₂S₂ ligands, the dianionic **Ni(ema)**²⁻ ligand significantly enriches the W(CO)₄ moiety with electron density as contrasted to the neutral analogues. Interestingly, the average $\nu(\text{CO})$ for [**Ni(ema)**W(CO)₄]²⁻ (1867 cm⁻¹) is only 18 cm⁻¹ lower than the average $\nu(\text{CO})$ values of the neutral complexes (1885 cm⁻¹). In contrast, the average $\nu(\text{CO})$ value of a dianionic dithiolate, (S,S-C₆H₄)W(CO)₄²⁻, is 1850 cm⁻¹ and that for a dithioether, (Bu'S(CH₂)₂SBu')W(CO)₄, is 1920 cm⁻¹, a 70 cm⁻¹ difference.^{52,53} In summary, the electron density transferred to the W(CO)₄ unit from the various bidentate S-donors is ranked as follows and denotes the buffer effect of

(52) Dobson, G. R. *Inorg. Chem.* **1969**, *8*, 90–95.

(53) Darensbourg, D. J.; Draper, J. D.; Frost, B. J.; Reibenspies, J. H. *Inorg. Chem.* **1999**, *38*, 4705–4714.

Ni(II) on the anionic S-donor.



Electrochemical studies find significant differences in accessibility of the Ni^{II/I} redox couple in the NiN₂S₂ metalthiolate ligands upon coordination of the thiolate sulfur's lone pairs to an exogenous metal. The differences in reduction potential appear to be more ligand dependent than are the $\nu(\text{CO})$ and force constant values. Hence, while the IR spectroscopic analysis finds no differences in donor ability of the neutral NiN₂S₂ metalthiolate ligands, the Ni^{II/I} redox couples, specifically the difference between the $E_{1/2}$ of the Ni^{II/I} couple in the free NiN₂S₂ ligand versus that bound to W(CO)₄, suggest the order of electron withdrawal from the NiN₂S₂ ligands by W(CO)₄ to be

Ni(bme-Me₂PDA) > Ni(bmmp-dmed) >

Ni-1' > Ni-1 ≈ Ni-1*

Interestingly, there is a significant, and as of now ill-defined, correlation of the hinge angles with the differences in $\Delta E_{1/2}$ of the Ni^{II/I} redox couples ($\Delta E_{1/2} = E_{1/2}(\text{Ni}^{\text{II/I}} \text{ of NiN}_2\text{S}_2\text{W}(\text{CO})_4) - E_{1/2}(\text{Ni}^{\text{II/I}} \text{ of NiN}_2\text{S}_2)$), the understanding of which will require computational chemistry.

Notably, the dianionic Ni(ema)²⁻ complex, that which most faithfully models the Ni(Cys-Gly-Cys) moiety in the ACS enzyme, was found within our series to most prominently display the property of hemilability, releasing one S–W bond and opening up a site on the W(CO)₄ moiety for the uptake of CO, producing a W(CO)₅ complex in which the NiN₂S₂²⁻ ligand is monodentate. This observation is consistent with the *in silico* mechanism for the ACS enzyme active site in which the Ni(Cys-Gly-Cys)²⁻ ligand switches into a monodentate form to accommodate addition of CO and switches back to re-form the resting state of the enzyme.^{8,9} Another interesting feature of the dianionic Ni(ema)²⁻ complex ligand is how easily it fits into the overall spectroscopic and reactivity pattern of the neutral NiN₂S₂ ligands. This result is compatible with the work of Hegg et al., which demonstrated an array of electrophile reactivity

with Ni(ema)²⁻ that mirrored the S-based reactivity of neutral NiN₂S₂ complexes.¹⁹ Consistent with these similarities is the small change in $\nu(\text{CO})$ stretching frequencies of the W(CO)₄ derivatives of the dianionic as compared to the neutral nickel–dithiolato complexes described above. Thus, in addition to moderation of charge by the nickel ion, it appears to buffer the donor ability.

For the purposes of synthetic design and for analysis of donor properties, we have treated the NiN₂S₂ complexes as “innocent” ligands.⁵⁴ This very useful assumption is arguably correct for the firm binding site for nickel in the tetradentate, square planar N₂S₂ coordination environment in combination with soft and low-valent metals, such as W⁰, Pd²⁺, and Ni^(II/0). It provides a rationale for the assembly of the ACS active site, a rationale that can possibly be extended to other binuclear active sites in biology and presumably in organometallic applications. However, whether this innocence will be maintained in combination with all metals is not known. The full potential of these ligands should be addressed through systems designed to take advantage of their unique properties, some of which we have identified, and some of which await further studies.

Acknowledgment. We gratefully acknowledge the financial support from the National Science Foundation (CHE 01-11629 and CHE 02-34860), Robert A. Welch Foundation, and the National Institutes of Health for a the Ruth L. Kirschstein-NRSA fellowship (to M.V.R., F31 GM073350-01). We appreciate a gift of the Ni(bmmp-dmed) from Dr. Craig A. Grapperhaus, University of Louisville.

Supporting Information Available: Additional syntheses of (NiN₂S₂)W(CO)₄ complexes; X-ray crystallographic files in CIF format for the structure determination of complexes 4–7. This material is available free of charge via the Internet at <http://pubs.acs.org>.

JA055051G

(54) The term “innocent” in this case refers to the stability of the Ni^{II} and RS⁻ redox levels throughout the reactions explored. However, the combination of a redox-active metal and thiolate sulfurs lends caution to this assumption. Ray, K.; Weyhermüller, T.; Neese, F.; Wieghardt, K. *Inorg. Chem.* **2005**, *44*, 5345–5360.